Inorganic Chemistry

Article

pubs.acs.org/IC

Highly Selective CO_2 Adsorption Accompanied with Low-Energy Regeneration in a Two-Dimensional Cu(II) Porous Coordination Polymer with Inorganic Fluorinated PF_6^- Anions

Shin-ichiro Noro,*[,†,‡,§] Yuh Hijikata,[∥] Munehiro Inukai,[⊥] Tomohiro Fukushima,[∥] Satoshi Horike,[∥] Masakazu Higuchi,[⊥] Susumu Kitagawa,[‡,∥,⊥] Tomoyuki Akutagawa,[#] and Takayoshi Nakamura*[,†]

[†]Research Institute for Electronic Science, Hokkaido University, Sapporo 001-0020, Japan

[‡]RIKEN SPring-8 Center, Kouto, Sayo-cho, Sayo-gun, Hyogo 679-5198, Japan

[§]PRESTO, Japan Science and Technology Agency (JST), 4-1-8 Honcho Kawaguchi, Saitama 332-0012, Japan

[∥]Department of Synthetic Chemistry & Biological Chemistry, Graduate School of Engineering, Kyoto University, Katsura, Nishikyo-ku, Kyoto 615-8510, Japan

[⊥]Institute for Integrated Cell-Material Science, Kyoto University, 69 Konoe-cho, Yoshida, Sakyo-ku, Kyoto 606-8501, Japan

[#]Institute for Multidisciplinary Research for Advanced Materials (IMRAM), Tohoku University, 1-1 Katahira, Aoba-ku, Sendai 980-8577, Japan

Supporting Information

ABSTRACT: High selectivity and low-energy regeneration for adsorption of CO_2 gas were achieved concurrently in a two-dimensional Cu(II) porous coordination polymer, $[Cu(PF_6)_2(4,4'\text{-bpy})_2]_n$ (4,4′-bpy = 4,4′-bipyridine), containing inorganic fluorinated PF_6^- anions that can act as moderate interaction sites for CO_2 molecules.

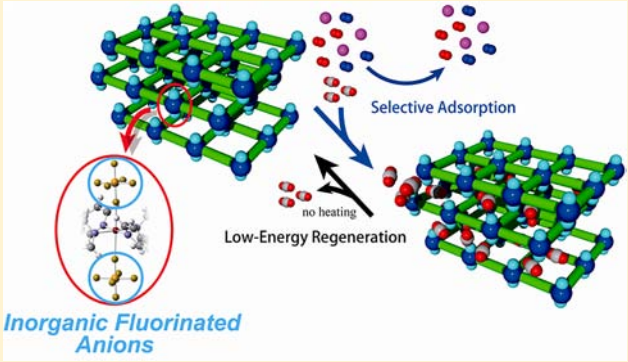

INTRODUCTION

Development of porous materials for selective adsorption of CO_2 gas from gas mixtures has been a significant challenge in natural-gas and biogas processing and exhaust gas treatment from power plants. CO_2 capture by porous materials is much more energy efficient than capture by chemical absorbents because physical adsorption requires less energy for regeneration. However, the traditional activated carbon materials are limited by low selectivities (for example, CO_2/N_2 selectivities are ca. 10), and while zeolites show considerably higher selectivities, they still suffer from high recovery cost for their regeneration. Hence, a key issue is balancing a strong affinity for removing an undesired component from a gas mixture with the energy consumption required for regeneration. Porous coordination polymers (PCPs) or metal−organic frameworks (MOFs) that are constructed from metal ions and organic bridging ligands are being intensively investigated to address this challenge because their metrics and chemical functionality can be carefully regulated for specific applications by appropriate combinations of building units, modification of organic ligands, control of crystal morphology, and hybridization.[1,2]

The conventional methods of offering high selectivity for CO_2 gas in PCP frameworks have included introducing (i) amine groups into organic ligands and (ii) coordinatively unsaturated metal cation centers that act as Lewis-base and Lewis-acid sites, respectively.[3,4] However, the interactions between these adsorption sites and CO_2 molecules are often too strong to release the CO_2 molecules under mild conditions. Therefore, it is very important to improve adsorption sites for CO_2 gas for practical use. Herein, we report the excellent CO_2 adsorption properties of two-dimensional PCP $[Cu(PF_6)_2(4,4'\text{-bpy})_2]_n$ (**1**; 4,4′-bpy = 4,4′-bipyridine) featuring inorganic fluorinated PF_6^- anions as moderate interaction sites for CO_2, which realize both high selectivity and low-energy regeneration. Although metal cations and organic ligands have been intensively used as building blocks providing CO_2 adsorption sites, examples of the application of inorganic anions are very few. To introduce such inorganic fluorinated PF_6^- anions efficiently into the porous framework we utilized a Cu(II) PCP

Received: August 21, 2012
Published: December 18, 2012

   dx.doi.org/10.1021/ic301823j | *Inorg. Chem.* 2013, 52, 280−285

framework capable of catching a variety of inorganic anions with weak Lewis-base properties at the Cu(II) axial sites.[5]

EXPERIMENTAL SECTION

Synthesis of 1⊃4MeOH. $AgPF_6$ (1.01 g, 4.00 mmol) was added to 10 mL of a MeOH solution containing $CuCl_2 \cdot 2H_2O$ (0.340 g, 2.00 mmol). The obtained suspension was stirred for 30 min and then filtered and washed with 10 mL of MeOH. To the sky blue filtrate, 10 mL of a MeOH solution containing 4,4′-bpy (0.624 g, 4.00 mmol) was added. The obtained purple microcrystals were filtered, washed with MeOH, and dried in vacuo at 298 K. Yield 85.7%. Anal. Calcd for **1** ($C_{20}H_{16}Cu_1F_{12}N_4P_2$): C, 36.08; H, 2.42; N, 8.41. Found: C, 36.03; H, 2.86; N 8.51.

X-ray Structural Analysis. X-ray diffraction measurement on **1**⊃4MeOH was performed using a Rigaku RAXIS-RAPID imaging plate diffractometer using graphite-monochromated Mo Kα radiation (λ = 0.71073 Å). Data were corrected for Lorentz and polarization effects. The structure was solved using direct methods (SIR2004)[6] and expanded using Fourier techniques. All non-hydrogen atoms were refined anisotropically. All hydrogen atoms were refined using the riding model. Refinements were carried out using full-matrix least-squares techniques on F^2. All calculations were performed using the CrystalStructure[7] crystallographic software package except for refinement, which was performed using SHELXL-97.[8] In the crystal structure, one guest MeOH was highly disordered even at 173 K. Therefore, the SQUEEZE function of PLATON[9] was used to eliminate the contribution of the electron density in the solvent region from the intensity data, and the solvent-free model of $\{[Cu(PF_6)(4,4'\text{-bpy})_2(MeOH)]\cdot PF_6\cdot 2MeOH\}_n$ was employed for the final refinement. The number of guest MeOH molecules in the pores was confirmed by the adsorption isotherms of MeOH at 298 K (see Figure S10, Supporting Information). Crystal data are summarized in Table S1, Supporting Information. CCDC-852811 contains the supplementary crystallographic data for this paper. Data can be obtained free of charge from The Cambridge Crystallographic Data Centre via www.ccdc.cam.ac.uk/data_request/cif.

Physical Measurements. Elemental analysis (C, H, and N) was performed using a PerkinElmer model 240C elemental analyzer. Solid-state MAS ^{31}P NMR spectra were measured by a Bruker Avance III 400 NMR spectrometer. Spectra were recorded at a resonance frequency of 161.97 MHz and a spinning rate of 12 or 7 kHz. The ^{31}P chemical shift was referenced to $(NH_4)_2HPO_4$. Thermogravimetric analyses were performed using a Rigaku Thermo Plus TG8120 apparatus in the temperature range between 298 and 773 K in a N_2 atmosphere and at a heating rate of 10 K min^{-1}. CO_2 cycling experiments were performed on the aforementioned analyzer using pure CO_2 (99.99%) and N_2 (99.999%). A flow rate of 50 mL min^{-1} was employed for both gases. Prior to cycling, samples were activated by heating at 353 K for 30 min, followed by cooling to 301 K under a N_2 atmosphere. Masses were uncorrected for buoyancy effects. As confirmed by the cycling experiment for $[Cu(PF_6)_2(4\text{-methylpyridine})_4]$ that shows no CO_2 and N_2 adsorption at near room temperature,[5c] the buoyancy effects were small compared to mass changes realized from gas adsorption. Mass changes due to buoyancy effects were observed when the gases were switched. XRD data of microcrystal samples were collected on a Rigaku Smartlab diffractometer with Cu Kα radiation. Adsorption isotherms were measured with BELSORP-max volumetric adsorption equipment. Before measurements, the sample was heated at 373 K under reduced pressure ($<10^{-2}$ Pa) for more than 8 h.

Calculations. Geometry optimization of the model complex $[Cu(PF_6)_2(pyridine)_4]$ with CO_2 was carried out by DFT with the M06-2X functional.[10] The basis set of Stuttgart-Dresden-Bonn (SDD) was used for Cu, where core electrons were replaced with the effective core potentials of SDD. 6-311+G-(d), 6-31G-(d), and 6-311G-(d) were employed for F, C, and H in pyridine and other atoms, respectively. The crystallographic structure of $[Cu(PF_6)_2(pyridine)_4]$ was used as an initial structure,[11] and the initial position of a CO_2 molecule was determined according to the literature to optimize whole this model system.[12] The interaction energy was evaluated at the DFT/M06-2X level with counterpoise corrections. All calculations were performed using the Gaussian 09 package.[13] The value of the interaction energy was corrected in consideration of a structural change of $[Cu(PF_6)_2(pyridine)_4]$.

RESULTS AND DISCUSSION

Reaction of $Cu(PF_6)_2$ with 4,4′-bpy in a MeOH solution at room temperature afforded $\{[Cu(PF_6)(4,4'\text{-bpy})_2(MeOH)]\cdot PF_6\cdot 3MeOH\}_n$ (**1**⊃4MeOH) as blue crystals. The crystal structure is shown in Figure 1, in which the Cu(II)

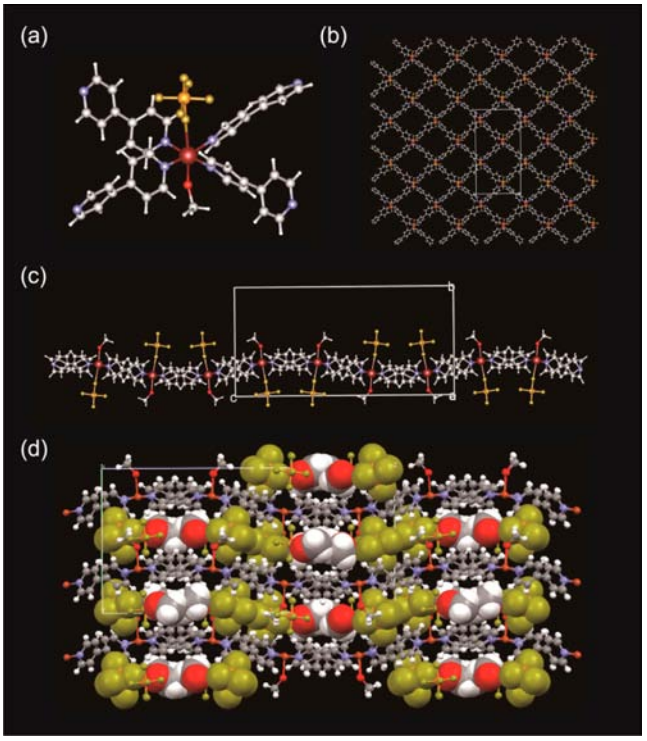

Figure 1. Crystal structure of **1**⊃4MeOH. (a) Coordination environment around the Cu(II) ion. (b and c) Two-dimensional layer structure in the projection along the (b) *b* and (c) *a* axis. (d) Packing structure viewed along the *a* axis. Coordination-free PF_6^- anions and MeOH guests are represented by a space-filling model. Vermilion represents copper, blue nitrogen, gray carbon, red oxygen, white hydrogen, gold fluorine, and orange phosphorus.

center has the elongated octahedral environment with four 4,4′-bpy nitrogen atoms in the basal plane and one MeOH oxygen atom and one PF_6^- fluorine atom at the axial sites (Cu−O and Cu−F distances = 2.306(3) and 2.614(3) Å). The 4,4′-bpy ligands bridge the Cu(II) centers to form two-dimensional undulating layers on the *ac* plane. Coordination-free PF_6^- anions and MeOH molecules are sandwiched between the layers. The accessible void space after removal of all MeOH molecules, calculated by the PLATON program, is 41%.[9] The calculated pore volume is 0.34 $cm^3\ g^{-1}$.

This PCP easily loses all guest MeOH molecules. Our previous report showed that originally uncoordinated PF_6^- anions can approach and weakly coordinate to the axial sites of Cu(II) centers after removal of the axially coordinated guest molecules.[5b,c] Hence, to obtain the coordination information for PF_6^- anions after removal of guest MeOH molecules, solid-state magic angle spinning (MAS) ^{31}P NMR spectra were measured. In general, the ^{31}P NMR spectra of the PF_6^- anion

dx.doi.org/10.1021/ic301823j | Inorg. Chem. 2013, 52, 280−285

have a septet pattern caused by the spin−spin coupling of the ^{19}F nucleus ($I = 1/2$) with the ^{31}P nucleus. In desolvated **1**, the observed spectra have two kinds of signals as shown in Figure 2: (a) a sharp septet and (b) broad ones at −145 and −189

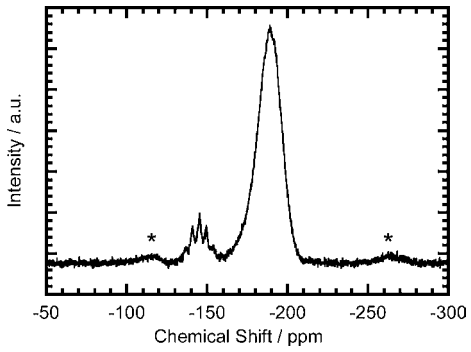

Figure 2. Solid state MAS ^{31}P NMR spectra in **1** at 298 K. Peaks denoted with the asterisks are the spinning sidebands.

ppm, respectively, with the area ratio of 1 to 10. The broad signal is also observed in the discrete complex $[Cu(PF_6)_2(4\text{-methylpyridine})_4]$ with weakly coordinated PF_6^- anions (−174 ppm, see Figure S1, Supporting Information).[5c] Therefore, the broadening is attributed to the effect of the paramagnetic Cu(II) ions in weakly coordinated PF_6^- anions. The presence of coordinated PF_6^- anions was also confirmed by the temperature-dependent solid-state MAS ^{31}P NMR spectra (Figure S2, Supporting Information), in which only the broad signal shows the temperature-dependent peak shift.[14] These results support the hypothesis that most of the originally uncoordinated PF_6^- anions weakly coordinate to the open axial sites formed after removal of coordinated MeOH molecules and that desolvated **1** possesses both uncoordinated and weakly coordinated PF_6^- anions in the ratio of 1 to 10, respectively.

The X-ray diffraction (XRD) pattern of desolvated **1** obtained by heating at 373 K under reduced pressure shows that desolvated **1** retains its crystallinity, but the positions of the peaks are different from those of the simulated XRD pattern in **1**⊃4MeOH (Figure S3, Supporting Information), supporting the changes in the assembled structure after removal of coordinated and free MeOH guests. The LeBail fitting for the XRD pattern (Figure S11, Supporting Information) indicates that removal of MeOH leads to a contraction of the interlayer distance.

To investigate the fundamental porous properties, we first measured the adsorption/desorption isotherms for N_2, O_2, Ar, and CO_2 at low temperature after removal of guest molecules at 373 K under vacuum (the pretreatment condition was determined from the thermogravimetric analysis (Figure S4, Supporting Information)). The microporous parameters are listed in Table S2, Supporting Information. The adsorption and desorption isotherms for N_2, O_2, Ar, and CO_2 represent similar stepwise curves, as shown in Figure 3. Such behaviors are similar to those observed in the analog $[Cu(CF_3SO_3)_2(4,4'\text{-bpy})_2]_n$,[15] which has an analogous two-dimensional framework with weakly coordinated $CF_3SO_3^-$ anions, that is, the first uptake is a micropore filling, while the second uptake originates from a gate-opening process (gate-opening pressures (P/P_0) are 2×10^{-2}, 4×10^{-2}, 5×10^{-2}, and 6×10^{-2} for N_2, O_2, Ar, and CO_2, respectively).[16] In $[Cu(CF_3SO_3)_2(4,4'\text{-bpy})_2]_n$, the gate-opening adsorption leads to an expansion of the interlayer

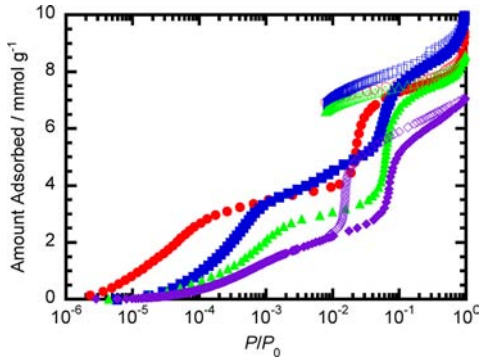

Figure 3. Adsorption (filled symbols) and desorption (open symbols) isotherms for N_2 (red, 77 K), O_2 (blue, 77 K), Ar (green, 77 K), and CO_2 (purple, 195 K) in **1**.

distance and a sliding between the layers.[15a] Similar structural transformations to the analog may also occur in the desolvated **1**, and therefore, a detailed structural analysis is a matter of ongoing work in our laboratory. The micropore volumes in the first step, calculated using the Dubinin−Radushkevich equation, are 0.15, 0.15, 0.10, and 0.092 $cm^3\ g^{-1}$ for N_2, O_2, Ar, and CO_2, respectively. The micropore volume of Ar is smaller than those of N_2 and O_2. Because the size in minimum dimension of Ar is larger than those of N_2 and O_2 (Lennard−Jones parameters of Ar 3.40 Å, N_2 3.32 Å, and O_2 3.11 Å),[17] this difference means that the larger size of Ar causes a slow diffusion into the pores. On the other hand, the micropore volume of CO_2 is considerably smaller than those of N_2 and O_2 despite the smaller size of CO_2 (Lennard−Jones parameter of CO_2 2.98 Å).[17] This may be because, compared with other gases, CO_2 with its larger quadrupole moment and polarizability relatively strongly (although the absolute value of Q_{st} is not as high, as we will discuss later) interacts with the permanent pores containing inorganic fluorinated PF_6^- anions, hardly diffusing deep into the pores. The micropore volume calculated from the N_2 adsorption data is considerably smaller than that calculated from single-crystal X-ray data (0.34 $cm^3\ g^{-1}$), because the assembled framework shrunk after removal of MeOH guests.

The CO_2, N_2, O_2, Ar, and CH_4 adsorption isotherms at 278 K are compared in Figure 4. **1** adsorbs very few N_2, O_2, and Ar and shows a small amount of adsorption for CH_4 at 278 K. On the other hand, the uptake of CO_2 at 100 kPa is ∼15 times higher than the uptake of N_2. The selectivity for adsorption of CO_2 over N_2, O_2, Ar, and CH_4 is a prerequisite for application

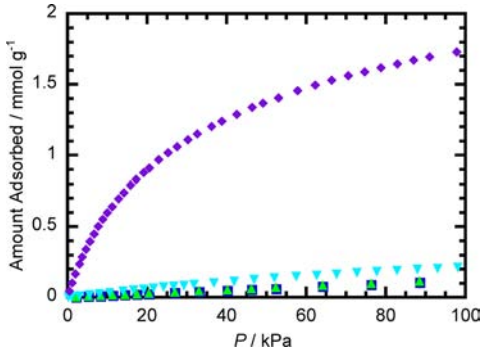

Figure 4. Adsorption isotherms for N_2 (red), O_2 (blue), Ar (green), CH_4 (sky blue), and CO_2 (purple) in **1** at 278 K. Because the amounts adsorbed for N_2, O_2, and Ar are almost the same, the symbols overlap.

dx.doi.org/10.1021/ic301823j | Inorg. Chem. 2013, 52, 280−285

of a framework as a separation material. Adsorption of gas mixtures in porous materials can be reliably estimated from single-component adsorption isotherms.[18] Hence, we determined the initial slopes in the Henry region of the adsorption isotherms of **1** (Figures S5 and S6, Supporting Information). The ratios of the slopes were used to estimate the adsorption selectivity for CO_2 over N_2, O_2, Ar, and CH_4. From these data, the CO_2/N_2 selectivity of 59:1 at 278 K (37:1 at 298 K) is comparable with the highest selectivity reported previously at a similar temperature.[19] The CO_2/O_2 and CO_2/Ar selectivities were 67:1 and 53:1 at 278 K, respectively, higher than those of other PCPs/MOFs and carbon materials.[20] The CO_2/CH_4 selectivity is 24:1 at 278 K. Although the high CO_2/CH_4 selectivities have been reported in (i) Mg-MOF-74 (330:1 at 298 K) with open Mg(II) cation sites that act as "end-on" binding sites for CO_2 molecules[21a] and (ii) amino-MIL-53 (almost infinite selectivity at 100 kPa and 303 K) functionalized with amino groups,[21b] **1** shows higher CO_2/CH_4 selectivity than those of zeolites and PCPs without open metal cation sites.[21c−e] These data indicate that **1** can compete with the benchmark PCPs for highly selective CO_2 capture.[19−22] The reason for the high CO_2 selectivity is probably caused by small pores and moderate acid−base interaction between CO_2 and PF_6^- anions.[12] The effective interactions between other fluorinated anions and CO_2 molecules have been also reported in PCPs.[23]

Recently, Snurr et al. used five adsorbent evaluation criteria from the chemical engineering literature for the potential of PCPs/MOFs in CO_2 separation processes.[2d] We focus on flue gas separation, which is currently an important research area. The typical composition of flue gas, that is, the CO_2/N_2 ratio, is assumed to be 10:90, and the adsorption/desorption pressures are set to 100/10 kPa, respectively. On the basis of this condition, **1** was evaluated and compared with not only other PCPs/MOFs but also commercially available inorganic and organic adsorbents (see Table S3, Supporting Information). As shown in Table S3, Supporting Information, **1** has high working capacity (or regenerability) and selectivity in this condition, resulting in a high sorbent selection parameter (S) that combines the working capacity and the adsorption selectivity. The S value obtained (214) is higher than those of zeolites (163 for zeolite 5A and 128 for zeolite 13X) and one of the best among the PCPs/MOFs. Hence, **1** seems to be promising for flue gas separation using vacuum-swing adsorption.

The regenerability of the CO_2 adsorption process in **1** was measured at 298 K (Figure 5). Significantly, the CO_2 adsorption ability of **1** is maintained over repeated cycling, and the material can be regenerated by simple vacuum processing without additional heating, in contrast to zeolites, which require high temperatures for complete regeneration.[24] Furthermore, adsorbed CO_2 can be easily removed from the material under a N_2 gas stream (see Figure S7, Supporting Information). The material may thus be suitable for use as an adsorbent in vacuum-swing and pressure-swing adsorption processes for CO_2 capture.

The isosteric heat of CO_2 adsorption, Q_{st}, was calculated from the virial equation using adsorption data collected at 278, 288, and 298 K (see Figure S8, Supporting Information). Q_{st} remains constant at a mean value of 31 kJ mol^{-1} in the range of micropore filling as the degree of CO_2 loading varies (see Figure S9, Supporting Information). Note that this is higher than the enthalpy of liquefaction of CO_2 (17 kJ mol^{-1}) and slightly lower than that observed for adsorption on $[Cu_3(1,3,5\text{-}btc)_2]_n$ (1,3,5-btc^{3-} = 1,3,5-benzenetricarboxylate) with coordinatively unsaturated Cu(II) centers (35 kJ mol^{-1}) at zero coverage[25] and considerably lower than the values observed for zeolites such as NaX and Na-ZSM-5 at zero coverage (~50 kJ mol^{-1}).[26] Such a moderate Q_{st} value is strongly related to an implementation of low-energy regeneration for CO_2 separation.

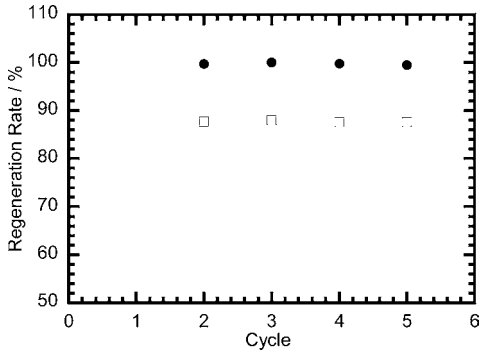

Figure 5. Regeneration rate as a function of CO_2 adsorption cycle for **1** (filled circles) and zeolite 13X (open squares) at 298 K. Rate was calculated according to the equation (amount adsorbed at 100 kPa in the nth cycle)/(amount adsorbed at 100 kPa in the first cycle) × 100.

As mentioned above, introduction of amine groups into organic ligands and coordinatively unsaturated metal cation centers on the surface of micropores has been universally applied to enhance adsorption selectivity for CO_2 gas. However, such sites strongly bind to CO_2 gas via acid−base interactions, preventing the CO_2 gas from escaping from the micropores in the regeneration process. The inorganic fluorinated PF_6^- anion employed in this study has been used as a counteranion of ionic liquids.[12,27] It is known that a CO_2 molecule interacts with this anion via an acid−base interaction in ionic liquids.[12,27c] Furthermore, we performed calculations of the geometry optimization of the model complex $[Cu(PF_6)_2(pyridine)_4]$[11] with a CO_2 molecule, and evaluated an interaction energy between the model complex and a CO_2 molecule. The optimized structure of $[Cu(PF_6)_2(pyridine)_4]$ with CO_2 is shown in Figure 6, in which the carbon atom of CO_2 lies in the plane formed by two P−F bond vectors of the weakly coordinated PF_6^- anion and the CO_2 molecule is perpendicular to this plane. The distances between the fluorine atoms and the carbon atom of CO_2 are 2.662 and 2.718 Å in

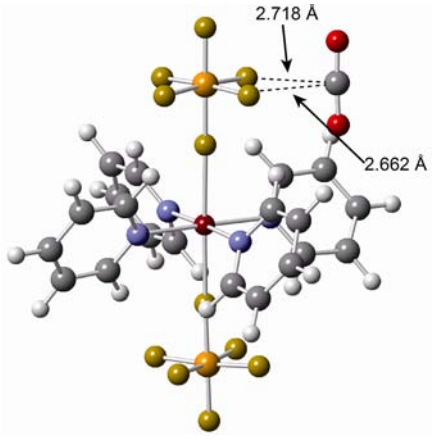

Figure 6. Optimized structure, obtained by DFT with M06-2X functional, of $[Cu(PF_6)_2(pyridine)_4]$ with CO_2.

dx.doi.org/10.1021/ic301823j | Inorg. Chem. 2013, 52, 280−285

the optimized structure and the interaction energy is found to be 28 kJ mol^{-1}, similar to the Q_{st} value calculated from the virial equation. These calculation results suggest that PF_6^- anions play a role of the preferable adsorption sites for CO_2. Hence, the observed moderate Q_{st} value and high selectivity in **1** can probably be attributed to interactions between inorganic fluorinated PF_6^- anions and CO_2 molecules.

CONCLUSIONS

We demonstrated the coexistence of high selectivity and low-energy regeneration for adsorption of CO_2 using the two-dimensional Cu(II) porous coordination polymer, $[Cu(PF_6)_2(4,4'\text{-bpy})_2]_n$ (**1**). The key point for success is to introduce the inorganic fluorinated PF_6^- anions with a very weak Lewis-base property to the Cu(II) axial sites in the framework for construction of high-performance CO_2 separating materials. Although amine groups on organic ligands and coordinatively unsaturated metal cation centers have been typically used for such a purpose, we achieved both high selectivity and low-energy regeneration by decorating the frameworks with inorganic fluorinated PF_6^- anions, which may cause the moderate interaction with CO_2 molecules. Work is in progress to improve the adsorption selectivity by precisely modifying organic bridging ligands of Cu(II) PCPs/MOFs having inorganic fluorinated anions within the framework.

ASSOCIATED CONTENT

Supporting Information

Solid-state MAS ^{31}P NMR spectra, XRD patterns, TG-DTA curves, detailed analysis of adsorption data, gas cycling experiments, and X-ray crystallographic data (CIF). This material is available free of charge via the Internet at http://pubs.acs.org.

AUTHOR INFORMATION

Corresponding Author

*E-mail: noro@es.hokudai.ac.jp (S.-i.N.); tnaka@es.hokudai.ac.jp (T.N.).

Notes

The authors declare no competing financial interest.

ACKNOWLEDGMENTS

We gratefully thank Prof. M. Kato, Prof. H.-C. Chang, and Dr. A. Kobayashi (Hokkaido University, Sapporo, Japan) for collecting temperature-dependent X-ray powder diffraction data. Computation time was provided by the SuperComputer System, Institute for Chemical Research, Kyoto University. This work was supported by PRESTO-JST and a Grant-in-Aid for Scientific Research, Young Scientists (B) (22750114), from MEXT, Japan.

REFERENCES

(1) (a) Kitagawa, S.; Kitaura, R.; Noro, S. *Angew. Chem., Int. Ed.* **2004**, *43*, 2334−2375. (b) Moulton, B.; Zaworotko, M. J. *Chem. Rev.* **2001**, *101*, 1629−1658. (c) Férey, G. *Chem. Soc. Rev.* **2008**, *37*, 191−214. (d) Wang, Z.; Cohen, S. M. *Chem. Soc. Rev.* **2009**, *38*, 1315−1329. (e) Song, Y.-F.; Cronin, L. *Angew. Chem., Int. Ed.* **2008**, *47*, 4635−4637. (f) Zacher, D.; Shekhah, L.; Wöll, C.; Fischer, R. A. *Chem. Soc. Rev.* **2009**, *38*, 1418−1429. (g) Horike, S.; Shimomura, S.; Kitagawa, S. *Nat. Chem.* **2009**, *1*, 695−704. (h) Shigematsu, A.; Yamada, T.; Kitagawa, H. *J. Am. Chem. Soc.* **2011**, *133*, 2034−2036. (i) Das, M. C.; Xiang, S.; Zhang, Z.; Chen, B. *Angew. Chem., Int. Ed.* **2011**, *50*, 10510−10520.

(2) (a) D'Alessandro, D. M.; Smit, B.; Long, J. R. *Angew. Chem., Int. Ed.* **2010**, *49*, 6058−6082. (b) Phan, A.; Doonan, C.; Uribe-Romo, F. J.; Knobler, C. B.; O'Keeffe, M.; Yaghi, O. M. *Acc. Chem. Res.* **2009**, *43*, 58−67. (c) Li, J.-R.; Ma, Y.; McCarthy, M. C.; Sculley, J.; Yu, J.; Jeong, H.-K.; Balbuena, P. B.; Zhou, H.-C. *Coord. Chem. Rev.* **2011**, *255*, 1791−1823. (d) Bae, Y.-S.; Snurr, R. Q. *Angew. Chem., Int. Ed.* **2011**, *50*, 11586−11596.

(3) (a) Demessence, A.; D'Alessandro, D. M.; Foo, M. L.; Long, J. R. *J. Am. Chem. Soc.* **2009**, *131*, 8784−8786. (b) Vaidhyanathan, R.; Iremonger, S. S.; Shimizu, G. K. H.; Boyd, P. G.; Alavi, S.; Woo, T. K. *Science* **2010**, *330*, 650−653.

(4) (a) Caskey, S. R.; Wong-Foy, A. G.; Matzger, A. J. *J. Am. Chem. Soc.* **2008**, *130*, 10870−10871. (b) Llewelln, P. L.; Bourrelly, S.; Serre, C.; Vimont, A.; Daturi, M.; Hamon, L.; Weireld, G.; Chang, J.-S.; Hong, D.-Y.; Hwang, Y. K.; Jhung, S. H.; Férey, G. *Langmuir* **2008**, *24*, 7245−7250.

(5) (a) Noro, S. *Phys. Chem. Chem. Phys.* **2010**, *12*, 2519−2531. (b) Noro, S.; Tanaka, D.; Sakamoto, H.; Shimomura, S.; Kitagawa, S.; Takeda, S.; Uemura, K.; Kita, H.; Akutagawa, T.; Nakamura, T. *Chem. Mater.* **2009**, *21*, 3346−3355. (c) Noro, S.; Ohba, T.; Fukuhara, K.; Takahashi, Y.; Akutagawa, T.; Nakamura, T. *Dalton Trans.* **2011**, *40*, 2268−2274. (d) Noro, S.; Kitaura, R.; Kondo, M.; Kitagawa, S.; Ishii, T.; Matsuzaka, H.; Yamashita, M. *J. Am. Chem. Soc.* **2002**, *124*, 2568−2583.

(6) SIR2004: Burla, M. C.; Caliandro, R.; Camalli, M.; Carrozzini, B.; Cascarano, G. L.; De Caro, L.; Giacovazzo, C.; Polidori, G.; Spagna, R. *J. Appl. Crystallogr.* **2005**, *38*, 381−388.

(7) *CrystalStructure 4.0.1: Crystal Structure Analysis Package*; Rigaku Corp.: Tokyo, Japan, 2000−2010.

(8) Sheldrick, B. M. *SHELXL-97: Program for the Refinement of Crystal Structure*; University of Göttingen: Germany, 1997.

(9) PLATON: Spek, A. L. *J. Appl. Crystallogr.* **2003**, *36*, 7−13.

(10) Zhao, Y.; Truhlar, D. G. *Theor. Chem. Acc.* **2008**, *120*, 215−241.

(11) Unpublished works.

(12) Bhargava, B. L.; Balasubramanian, S. *Chem. Phys. Lett.* **2007**, *444*, 242−246.

(13) Frisch, M. J.; Trucks, G. W.; Schlegel, H. B.; Scuseria, G. E.; Robb, M. A.; Cheeseman, J. R.; Scalmani, G.; Barone, V.; Mennucci, B.; Petersson, G. A.; Nakatsuji, H.; Caricato, M.; Li, X.; Hratchian, H. P.; Izmaylov, A. F.; Bloino, J.; Zheng, G.; Sonnenberg, J. L.; Hada, M.; Ehara, M.; Toyota, K.; Fukuda, R.; Hasegawa, J.; Ishida, M.; Nakajima, T.; Honda, Y.; Kitao, O.; Nakai, H.; Vreven, T.; Montgomery, Jr., J. A.; Peralta, J. E.; Ogliaro, F.; Bearpark, M.; Heyd, J. J.; Brothers, E.; Kudin, K. N.; Staroverov, V. N.; Kobayashi, R.; Normand, J.; Raghavachari, K.; Rendell, A.; Burant, J. C.; Iyengar, S. S.; Tomasi, J.; Cossi, M.; Rega, N.; Millam, J. M.; Klene, M.; Knox, J. E.; Cross, J. B.; Bakken, V.; Adamo, C.; Jaramillo, J.; Gomperts, R.; Stratmann, R. E.; Yazyev, O.; Austin, A. J.; Cammi, R.; Pomelli, C.; Ochterski, J. W.; Martin, R. L.; Morokuma, K.; Zakrzewski, V. G.; Voth, G. A.; Salvador, P.; Dannenberg, J. J.; Dapprich, S.; Daniels, A. D.; Farkas, Ö.; Foresman, J. B.; Ortiz, J. V.; Cioslowski, J.; Fox, D. J. *Gaussian 09*; Gaussian, Inc.: Wallingford, CT, 2009.

(14) Haw, J. F.; Campbell, G. C. *J. Magn. Reson.* **1986**, *66*, 558−561.

(15) (a) Kondo, A.; Noguchi, H.; Carlucci, L.; Proserpio, D. M.; Ciani, G.; Kajiro, H.; Ohba, T.; Kanoh, H.; Kaneko, K. *J. Am. Chem. Soc.* **2007**, *129*, 12362−12363. (b) Kondo, A.; Kajiro, H.; Noguchi, H.; Carlucci, L.; Proserpio, D. M.; Ciani, G.; Kato, K.; Takata, M.; Seki, H.; Sakamoto, M.; Hattori, Y.; Okino, F.; Maeda, K.; Ohba, T.; Kaneko, K.; Kanoh, H. *J. Am. Chem. Soc.* **2011**, *133*, 10512−10522. (c) Kondo, A.; Chinen, A.; Kajiro, H.; Nakagawa, T.; Kato, K.; Takata, M.; Hattori, Y.; Okino, F.; Ohba, T.; Kaneko, K.; Kanoh, H. *Chem.—Eur. J.* **2009**, *15*, 7549−7553.

(16) (a) Kondo, A.; Noguchi, H.; Ohnishi, S.; Kajiro, H.; Tohdoh, A.; Hattori, Y.; Xu, W.-C.; Tanaka, H.; Kanoh, H.; Kaneko, K. *Nano Lett.* **2006**, *6*, 2581−2584. (b) Kitaura, R.; Seki, K.; Akiyama, G.; Kitagawa, S. *Angew. Chem., Int. Ed.* **2003**, *42*, 428−431. (c) Bourrelly, S.; Llewellyn, P. L.; Serre, C.; Millange, F.; Loiseau, T.; Férey, G. *J. Am. Chem. Soc.* **2005**, *127*, 13519−13521. (d) Hijikata, Y.; Horike, S.; Sugimoto, M.; Sato, H.; Matsuda, R.; Kitagawa, S. *Chem.—Eur. J.*

2011, *17*, 5138−5144. (e) Shimomura, S.; Higuchi, M.; Matsuda, R.; Yoneda, K.; Hijikata, Y.; Kubota, Y.; Mita, Y.; Kim, J.; Takata, M.; Kitagawa, S. *Nat. Chem.* **2010**, *2*, 633−637.
(17) Vrabec, J.; Stoll, J.; Hasse, H. *J. Phys. Chem. B* **2001**, *105*, 12126−12133.
(18) (a) Myers, A. L.; Prausnitz, J. M. *AIChE J.* **1965**, *11*, 121−127. (b) Bae, Y.-S.; Farha, O. K.; Spokoyny, A. M.; Mirkin, C. A.; Hupp, J. T.; Snurr, R. Q. *Chem. Commun.* **2008**, 4135−4137. (c) Bae, Y.-S.; Farha, O. K.; Hupp, J. T.; Snurr, R. Q. *J. Mater. Chem.* **2009**, *19*, 2131−2134.
(19) (a) Henke, S.; Fischer, R. A. *J. Am. Chem. Soc.* **2011**, *133*, 2064−2067. (b) An, J.; Geib, S. J.; Rosi, N. L. *J. Am. Chem. Soc.* **2010**, *132*, 38−39.
(20) Banerjee, R.; Furukawa, H.; Britt, D.; Knobler, C.; O'Keeffe, M.; Yaghi, O. M. *J. Am. Chem. Soc.* **2009**, *131*, 3875−3877.
(21) (a) Britt, D.; Furukawa, H.; Wang, B.; Glover, T. G.; Yaghi, O. M. *Proc. Natl. Acad. Sci. U.S.A.* **2009**, *106*, 20637−20640. (b) Couck, S.; Denayer, J. F. M.; Varon, G. V.; Rémy, T.; Gascon, j.; Kapteijn, F. *J. Am. Chem. Soc.* **2009**, *131*, 6326−6327. (c) Bae, Y.-S.; Mulfort, K. L.; Frost, H.; Ryan, P.; Punnathanam, S.; Broadbelt, L. J.; Hupp, J. T.; Snurr, R. Q. *Langmuir* **2008**, *24*, 8592−8598. (d) Cavenati, S.; Grande, C. A.; Rodrigues, A. E. *J. Chem. Eng. Data* **2004**, *49*, 1095−1101. (e) Li, P. Y.; Tezel, F. H. *Microporous Mesoporous Mater.* **2007**, *98*, 94−101.
(22) (a) An, J.; Geib, S. J.; Rosi, N. L. *J. Am. Chem. Soc.* **2010**, *19*, 2131−2134. (b) Demessence, A.; D'Alessandro, D. M.; Lin Foo, M.; Long, J. R. *J. Am. Chem. Soc.* **2009**, *131*, 8784−8786. (c) Wang, B.; Côte, A. P.; Furukawa, H.; O'Keeffe, M.; Yaghi, O. M. *Nature* **2008**, *453*, 207−212. (d) Vaidhyanathan, R.; Iremonger, S. S.; Dawson, K. W.; Shimizu, G. K. H. *Chem. Commun.* **2009**, 5230−5232. (e) Choi, H.-S.; Suh, M. P. *Angew. Chem., Int. Ed.* **2009**, *48*, 6865−6869.
(23) (a) Kanoo, P.; Reddy, S. K.; Kumari, G.; Haldar, R.; Narayana, C.; Balasubramanian, S.; Maji, T. K. *Chem. Commun.* **2012**, *48*, 8487−8489. (b) Burd, S. D.; Ma, S.; Perman, J. A.; Sikora, B. J.; Snurr, R. Q.; Thallapally, P. K.; Tian, J.; Wojtas, L.; Zaworotko, M. J. *J. Am. Chem. Soc.* **2012**, *134*, 3663−3666. (c) Uemura, K.; Maeda, A.; Maji, T. K.; Kanoo, P.; Kita, H. *Eur. J. Inorg. Chem.* **2009**, 2329−2337.
(24) Franchi, R. S.; Harlick, P. J. E.; Sayari, A. *Ind. Eng. Chem. Res.* **2005**, *44*, 8007−8013.
(25) Wang, Q. M.; Shen, D.; Bülow, M.; Lau, M. L.; Deng, S.; Fitch, F. R.; Lemcoff, N. O.; Semanscin, L. *Microporous Mesoporous Mater.* **2002**, *55*, 217−230.
(26) Dunne, J. A.; Rao, M.; Sircar, S.; Gorte, R. J.; Myers, A. L. *Langmuir* **1996**, *12*, 5896−5904.
(27) (a) Cammarata, L.; Kazarian, S. G.; Salter, P. A.; Welton, T. *Phys. Chem. Chem. Phys.* **2001**, *3*, 5192−5200. (b) Aki, S. N. V. K.; Mellein, B. R.; Saurer, E. M.; Brennecke, J. F. *J. Phys. Chem. B* **2004**, *108*, 20355−20365. (c) Kazarian, S. G.; Briscoe, B. J.; Welton, T. *Chem. Commun.* **2000**, 2047−2048.

dx.doi.org/10.1021/ic301823j | *Inorg. Chem.* 2013, 52, 280−285